Insights into Intermediate Phases of Human Intestinal Fluids Visualized by Atomic Force Microscopy and Cryo-Transmission Electron Microscopy *ex Vivo*

Anette Müllertz,[†] Dimitrios G. Fatouros,*[,‡] James R. Smith,[§] Maria Vertzoni,[‖] and Christos Reppas[‖]

[†]Bioneer:FARMA, Department of Pharmaceutics and Analytical Chemistry, The Faculty of Pharmaceutical Science, University of Copenhagen, Universitetsparken 2, 2100 Copenhagen, Denmark

[‡]Department of Pharmaceutical Technology, School of Pharmacy, Aristotle University of Thessaloniki, 54124, Greece

[§]School of Pharmacy and Biomedical Sciences, University of Portsmouth, St Michael's Building, White Swan Road, Portsmouth PO1 2DT, United Kingdom

[‖]Department of Pharmaceutical Technology, Faculty of Pharmacy, National and Kapodistrian University of Athens, Panepistimiopolis 15771 Zografou, Greece

ABSTRACT: The current work aims to study at the ultrastructural level the morphological development of colloidal intermediate phases of human intestinal fluids (HIFs) produced during lipid digestion. HIFs were aspirated near the ligament of Treitz early (30 min), $Aspirate_{early}$, and 1 h, $Aspirate_{1h}^{ave,comp}$, after the administration of a heterogeneous liquid meal into the antrum. The composition of the sample aspirated 1 h after meal administration was similar to the average lumenal composition 1 h after meal administration ($Aspirate_{1h}^{ave,comp}$). The colloidal structures of individual aspirates and supernatants of aspirates after ultracentrifugation (micellar phase) were characterized by means of atomic force microscopy (AFM) and cryogenic transmission electron microscopy (Cryo-TEM). AFM revealed domain-like structures in $Aspirate_{early}$ and both vesicles and large aggregates $Aspirate_{1h}^{ave,comp}$. Rough surfaces and domains varying in size were frequently present in the micellar phase of both $Aspirate_{early}$ and $Aspirate_{1h}^{ave,comp}$. Cryo-TEM revealed an abundance of spherical micelles and occasionally presented worm-like micelles coexisting with faceted and less defined vesicles in $Aspirate_{early}$ and $Aspirate_{1h}^{ave,comp}$. In $Aspirate_{1h}^{ave,comp}$ oil droplets were visualized with bilayers closely located to their surface suggesting lipolytic product phases accumulated on the surface of the oil droplet. In the micellar phase of $Aspirate_{early}$, Cryo-TEM revealed the presence of spherical micelles, small vesicles, membrane fragments, oil droplets and plate-like structures. In the micellar phase of $Aspirate_{1h}^{ave,comp}$, the only difference was the absence of oil droplets. Visualization studies previously performed with biorelevant media revealed structural features with many similarities as presented in the current investigation. The impression of the complexity and diversion of these phases has been reinforced with the excessive variation of structural features visualized *ex vivo* in the current study offering insights at the ultrastuctural level of intermediate phases which impact drug solubilization.

KEYWORDS: *human intestinal fluids (HIFs), atomic force microscopy (AFM), cryo-transmission electron microscopy (Cryo-TEM), lipid digestion, laser diffraction*
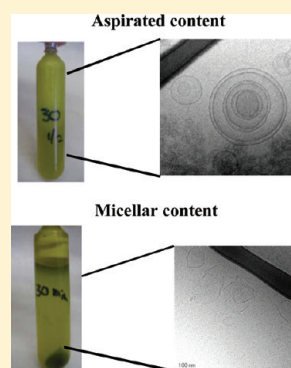
INTRODUCTION

The physicochemical nature of lipids in the gastrointestinal (GI) tract was first described in the early 1960s.[1,2] The liquid crystalline phases produced during lipid digestion was first confirmed by light microscopy.[3,4] Later, multilamellar phases were visualized with freeze fracture electron microscopy (FFEM) as rough surfaces with variable distance between the lamellae in *in vitro* systems with and without lipolysis products and on lipolytic colloidal phases produced in the intestine of the killfish after fat feeding.[5] In 1990, Staggers et al. demonstrated the existence of both micelles and unilamellar vesicles in both *in vivo* and *in vitro* samples from duodenal aspirates by quasielastic light scattering techniques.[6,7]

Intraluminal digestion of triglycerides, by gastric or pancreatic lipases, results in the generation of mainly monoacylglycerides and free fatty acids, which are believed to accumulate on the surface of oil droplets. Monoglycerides and fatty acids will facilitate the formation of multilamellar liquid crystalline phases on the surface droplet that are gradually "detached" from the surface and produce either multi- or unilamellar vesicles and finally, upon further interaction with bile salts, are transformed into mixed micelles.[5] Upon their formation on the surface of the oil droplets there are two ways for free fatty acids to be removed from the surface: either via the formation of calcium soaps or by being solubilized in mixed bile salt micelles. During lipid digestion, the trafficking of a particular drug between these various colloid phases will be

controlled by several factors, many of which are poorly understood, but are thought to include the drug lipophilicity and affinity for the various lipolytic phases.[8,9] An important question is to what extent these phases can modulate the transfer of the drug across different colloidal phases and into mixed micelles, which are believed to transport the drug to the unstirred water layer where they ultimately disintegrate and the drug is absorbed and eventually reaches the systemic circulation.

At present, there is a considerable interest in ultrastructural changes of these colloid phases during lipid digestion and different physical techniques, such as electron microscopy,[10−13] X-ray diffraction,[14,15] electron spin resonance,[16] and multiplex coherent anti-Stokes Raman scattering microspectroscopy,[17] have been employed to elucidate this. In the current study, human intestinal fluids (HIFs) were aspirated from healthy subjects and characterized *ex vivo* by means of atomic force microscopy (AFM) and cryogenic transmission electron microscopy (Cryo-TEM). AFM can provide information on the surface topology of these phases without the need for special sample processing; all investigations can be carried out in physiological conditions. AFM has been used before to investigate the domain structures of mixed lipid membranes.[18] On the other hand the advantage of Cryo-TEM is the avoidance of any fixation of the sample which reduces the possibility of artifacts induced by staining and eliminates the risk of extraction of lipid material.[19]

To the best of our knowledge, this is the first report utilizing AFM and Cryo-TEM, two minimally destructive methods, to visualize, at the ultrastructural level, the microenvironment of HIFs *ex vivo*.

■ MATERIALS AND METHODS

Origin of Samples. Samples of contents of the small intestine were aspirated from a location near the ligament of Treitz during a previous study performed that involved the administration of a standardized mixed meal of 750 kCal to healthy adults.[20] Each subject reported at the clinic in the morning fasted (for at least 12 h) and, if female, was tested for pregnancy. The subject was intubated nasally using a sterile two lumen duodenal tube (Freka Trelumina Ch/Fr 16/9, 150 cm, ref no. 7550911). The two lumen tube was 150 cm long with an external diameter of 5.3 cm. A series of holes (55−65 cm proximal to the end of the tube) were used to access the antrum of the stomach. A further series of handmade holes (13.5−23.5 cm proximal to the end of the tube) were used to aspirate samples from the lumen. The insertion of the tube was assisted by a guiding wire, and its position was monitored fluoroscopically. After reaching its final position and removing the wire, a heterogeneous liquid meal containing the drug was administered to the antrum using 60 mL (capacity) syringes. The meal contained 150 mg of danazol, 62.5 g of olive oil, 1.25 eggs, 25.0 g of sucrose, 2.7 g of sodium chloride, and vanilla flavor and was brought to a total volume of 500 mL upon addition of 356 mL of water,[20] following a similar meal composition used before.[21] Prior to the administration, the meal was vigorously mixed by mechanical blending for 10 s; this process was selected to generate a coarse emulsion.[20,21]

Since maximum changes of luminal composition after administration of the meal were observed during the first hour after administration,[20] we selected two samples aspirated within this period. One sample was aspirated from subject #1, 1 h after the administration of the meal, and the other sample was aspirated from subject #2, early (30 min) after meal administration. Immediately after aspiration, a cocktail of lipase/proteolysis inhibitors [2% (v/v)][6] was added, and each sample was divided in two subsamples. The first was kept at −70 °C. The second subsample was ultracentrifuged (410174 g, 37 °C, 2 h) so that four phases were observed, that is, oily phase, interface, micellar phase, and pellet.[6,22] After separation, the micellar phase was stored at −70 °C prior to the analysis.

The pH, buffer capacity, osmolality, and protein content were determined as described previously.[20] The determination of individual bile acids and glyceride contents in aspirates collected from the upper gastrointestinal lumen were quantified by applying liquid chromatography.[20,23,24]

Particle Size Analysis. The particle size distribution of the emulsion prior its administration was determined by laser diffraction analysis. Laser diffraction analysis was performed on a Malvern Mastersizer S equipped with a 300RF lens (Malvern Instruments, UK). The mean particle size was calculated from the volume size distribution.

Visualization Studies Protocol. One hour after meal administration, samples were collected from the first volunteer, and the total content and micellar phases were visualized by means of AFM and Cryo-TEM. In a similar manner 30 min following the meal, samples were collected from the second volunteer and processed for microscopy analysis.

AFM Studies. AFM studies (MultiMode/NanoScope IV scanning probe microscope, Digital Instruments, Santa Barbara, CA, USA) were performed in air under ambient conditions (T = 23 °C, RH = 21%) using the J-scanner (max. xy = 200 μm). Scanning was performed in tapping mode using Si cantilevers with integrated tips (t = 3.5−4.5 μm, l = 115−135 μm, w = 30−40 μm, ν_0 = 200−400 kHz, k = 20−80 N m^{-1}, R < 10 nm; model: RTESP, Veeco Instruments, France), and an rms amplitude of 0.8 V was used. The images were subsequently processed using NanoScope software (V 7.10, Digital Instruments, Santa Barbara, CA, USA). Specimens for imaging were prepared by placing a dispersion (10 μL) of each sample onto the freshly cleaved surface of muscovite mica (Agar Scientific, Stansted, Essex, UK; mounted on a nickel disk), leaving for 2 min and then drying the surface in a stream of N$_2$. Dimensions (heights and widths) of features were obtained from line-profiles using NanoScope software (V6.11r1, Bruker, Santa Barbara, CA, USA).

Cryo-TEM Studies. The samples for the Cryo-TEM studies were prepared in a controlled environment vitrification system (CEVS). A small amount of the sample (5 μL) was put on carbon film supported by a copper grid and blotted with filter paper to obtain a thin liquid film on the grid. The grid was quenched in liquid ethane at −180 °C and transferred to liquid nitrogen (−196 °C). The samples were characterized with a TEM microscope (Philips CM120 BioTWIN Cryo) equipped with a post column energy filter (GATAN GIF 100) using an Oxford CT3500 cryoholder and its workstation. The acceleration voltage was 120 kV, and the working temperature was −180 °C. The images were recorded with a charge-coupled device (CCD) camera (Gatan 791) under low dose conditions. The defocus was ca. 1 μm.

■ RESULTS

Particle Size Measurements. The droplet size distribution of the test meal is illustrated in Figure 1. The mean volume diameter [D (n, 0.5)] of the coarse emulsion was 1.21 ± 0.16 μm with oil droplets varying from 0.50 to 30.50 μm. Half of the
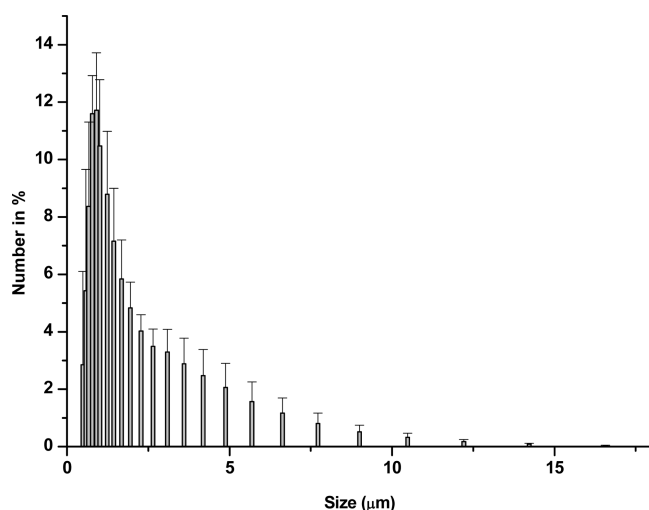
Figure 1. Number (%) versus particle size diameter (μm), measured using laser diffraction, of the emulsion administered to the volunteers ($n = 6$).

emulsified droplets (50.4% of the total number) were less than 1 μm in diameter. In 47.6% of the total number of the droplets the diameter spanned from 1 to 6.6 μm, whereas only 2% of the coarse emulsion was composed from oil droplets with diameters up to 22.5 μm.

HIFs Analysis. The physicochemical characteristics and composition of HIFs are shown in Table 1. The first sample (aspirated from subject #1, 60 min after the administration of the meal) and its micellar phase had a composition close to the average composition of HIFs and of their micellar phases 1 h after administration.[20] As shown in Table 1, the composition of micellar phase of this sample (Micellar$_{1h}^{ave,comp}$) is substantially different than the aspirated composition (Aspirate$_{1h}^{ave,comp}$). In contrast, in the second sample [aspirated from subject #2, early (30 min) after meal administration] the composition of micellar phase (Micellar$_{early}$) was practically similar to the composition of the aspirated sample (Table 1, Aspirate$_{early}$).

It should be emphasized that the low TG contents in the "early" sample does not mean that the sample is not representative of the fed state. Total bile salt concentrations of 6 mM and free fatty acid concentrations of 12 mM (Table 1) in the fasted upper SI are very rare.

AFM Analysis of HIFs. The micrographs selected are representative of 54 images in total.

Aspirate$_{1h}^{ave,comp}$ Sample. An abundance of spherical vesicles, with a mean height of 7.5 ± 2.6 nm ($n = 30$) and diameter of 98 ± 34 nm, were observed in the Aspirate$_{1h}^{ave,comp}$ sample (Figure 2A). The low height with respect to diameter may be due to the partial collapse of the vesicle under the imaging conditions employed. AFM measurements have shown dipalmitoylphosphatidylcholine (DPPC) single bilayers to have a thickness of ca. 5 nm,[25] which is similar to the vesicle height reported here. A few holes in the underlying lipid bilayer, as with the Aspirate$_{early}$ sample, were also seen. In addition, large aggregates with an irregular structure and grain texture were occasionally visible (Figure 2B). A height-section through these structures, corresponding to the line profile in Figure 2B, is shown in Figure 2C. A mean height of 15.9 nm was observed, which is about twice that of the 7.5 nm height, and hence may correspond to double bilayers coupled with partial vesicle collapse.

Aspirate$_{early}$ Sample. The Aspirate$_{early}$ sample shows the presence of circular features that are thought to be holes in the lipid bilayer on the mica surface (data not shown). These may have formed due to collapse of the vesicle structures.[25]

Micellar$_{1h}^{ave,comp}$ Sample. Domains varying in size were frequently present at the Micellar$_{1h}^{ave,comp}$, as depicted in Figure 3A. The contours of these domains were rough and had irregular shapes. A height analysis of membrane thickness (Figure 3B, corresponding to the line profile in Figure 3A) measured across different domains showed different heights (4.1, 4.6, and 11.0 nm depicted in Figure 3B), which implies the existence of more than one phase in the Micellar$_{1h}^{ave,comp}$ sample.

Micellar$_{early}$ Sample. In the Micellar$_{early}$ sample, a homogeneous condensed phase with some defects of molecular packing seen as small holes were observed (Figure 3C). A cluster with rough surfaces [possibly lamellae] (indicated by white arrows)

Table 1. Physicochemical Characteristics of Two Samples Aspirated near the Ligament of Treitz and of Their Micellar Phase after Administration of a Meal (750 kCal) to the Stomach of Fasted Healthy Adults[a]

	subject #1		subject #2	
	Aspirate$_{1h}^{ave,comp}$	Micellar$_{1h}^{ave,comp}$	Aspirate$_{early}$	Micellar$_{early}$
pH	5.15	N.M.	6.37	N.M.
buffer capacity (mmol/L/ΔpH)	10	N.M.	15	N.M.
osmolality (mOsmol/kg)	516	483	399	363
protein content (mg/mL)	7.43	5.09	4.00	2.58
total bile salts (mM)	2.654	4.066	6.453	5.873
free fatty acids (mM)	27.898	15.835	12.646	11.003
monoglycerides (mM)	3.842	0.418	0.238	0.922
diglycerides (mM)	5.707	0.481	0.483	0.198
triglycerides (mM)	16.654	<LOD	0.026	<LOD
lyso-phosphatidylcholine (mM)	1.755	1.908	2.538	2.436
phosphatidylcholine (mM)	3.298	0.185	0.254	0.153
cholesterol (mM)	1.115	0.589	1.013	1.392
LP/BS	11.95	3.99	1.99	2.03
PC/BS	1.90	0.51	0.43	0.44

[a]N.M., not measured; LOD, limit of detection; LP, lipolytic products (sum of free fatty acids, monoglycerides); BS, bile salts; PC, sum of phosphatidylcholine and lysophosphatidylcholine.
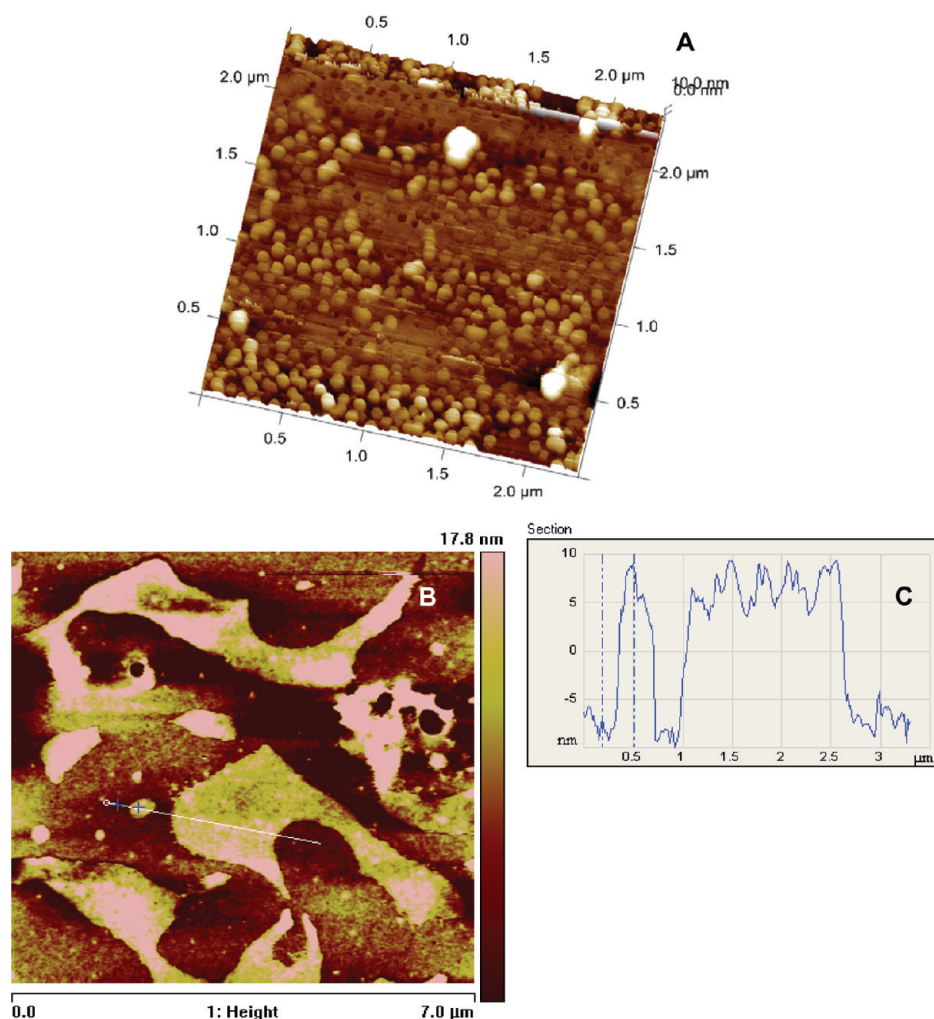
Figure 2. AFM images of HIFs. (A) Spherical vesicles with diameters ca. 70 nm of the Aspirate$_{1h}^{ave,comp}$ sample. (B) Aggregates with an irregular structure and grain texture of the Aspirate$_{1h}^{ave,comp}$ sample. (C) Height analysis of membrane thickness of the Aspirate$_{1h}^{ave,comp}$ sample (blue line height = 15.9 nm).

and channels (indicated by black arrows) were visible in this sample (Figure 3C).

Cryo-TEM Analysis of HIFs. The micrographs selected are representative of 128 images in total.

Aspirate$_{1h}^{ave,comp}$ Sample. When looking at the Aspirate$_{ave,comp}$ samples, bilamellar (Figure 4A, indicated by a black arrow) vesicles with diameters ranging between 100 and 200 nm and occasional concentric multilamellar vesicles with diameters up to 600 nm were visible (Figure 4A, indicated by a white arrow). It is noteworthy that the distance between the membranes of the pairs in the multilamellar vesicle (Figure 4A) is practically constant, implying periodicity and repulsive interaction as has been observed previously.[10,11]

Spherical micelles were always present in the background of the micrographs as tiny black dots (diameters of ca. 10 nm), and oil droplets were also present (Figure 4B and C, respectively). Figure 4B shows a submicrometer size emulsion droplet of ca. 300 nm coexisting with a bilamellar (indicated by dashed black arrow), a unilamellar (indicated by a black arrow), and a ruptured vesicle (indicated by a dashed white arrow), respectively. However, a very interesting finding was the presence of a bilayer fragment loosely associated with the surface of the oil droplet (Figure 4B, indicated by a white arrow). This observation is more pronounced in Figure 4C,

where protrusions (bilayers) emerged from the oil droplet with a particle size of ca. 600 nm (indicated by white arrows). These droplets have similarities with the reported oil droplets with rough texture surfaces previously visualized by freeze fracture electron microscopy during fat digestion.[5] The multiple layers of rough-textured lamellae were gradually detached from the droplet surfaces and formed unilamellar vesicles and mixed micelles.

Although it is difficult to claim unambiguously that the same phenomenon is witnessed in these micrographs, our data point to this direction.

Micellar$_{1h}^{ave,comp}$ Sample. In the micellar phase, no oil droplets could be detected, suggesting their gradual degradation to intermediate lipolytic products intraluminally.[5] Spherical micelles, with diameters ca. 10 nm, were the dominating structural features and unilamellar perforated vesicles were frequently present (Figure 5A, the latter indicated by a black arrow). Such openings inducing the creation of pores in lipid membranes indicate the pronounced effect of bile salts in the system.[11] Occasionally, bilayer fragments, aggregated material (possibly proteins originating from pancreatic lipase) (data not shown), and occasionally faceted vesicles with irregular structures (Figure 5B, indicated by white arrow) were visualized. Vesicles with edges, also called faceted vesicles,
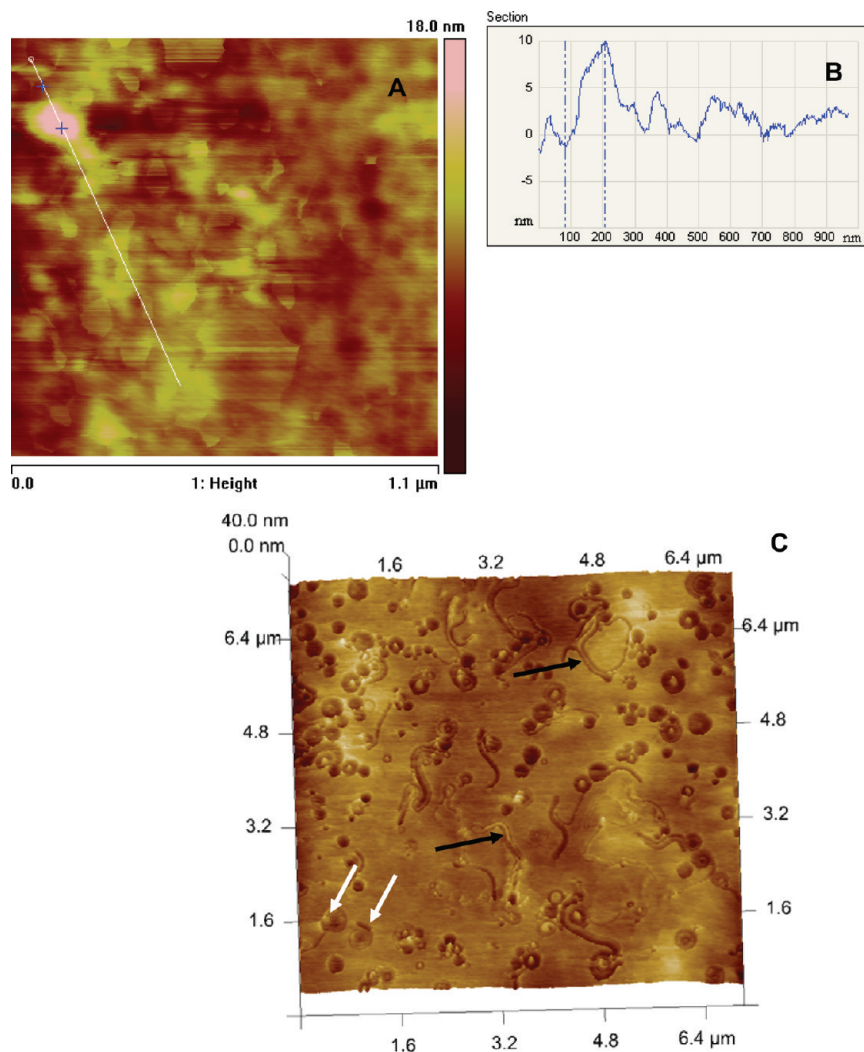
Figure 3. AFM images of micellar phase of HIFs. (A) Heterogeneous surface of the Micellar$_{1h}^{ave,comp}$ sample. (B) Height analysis of the Micellar$_{1h}^{ave,comp}$ surface showing various domain heights (blue line height = 11.0 nm, other main heights: 4.1 and 4.6 nm). (C) Rough surfaces (indicated by white arrows) and channels (indicated by black arrows) of the Micellar$_{early}$ sample micellar phase.

have been observed previously in other lipid mixtures[26] and milk membrane lipids.[27] The formation of faceted structures might be related to the uneven composition of the lipid material in or at the surface of the membrane.[25]

Aspirate$_{early}$ Sample. The structural changes became more pronounced in the Aspirate$_{early}$ sample (Figure 6). Both spherical micelles ca. 10 nm (Figure 6A, indicated by black dots) and thread-like micelles ca. 30 nm [in length] (Figure 6B) were frequently observed in the sample. The thread-like micelles visualized in the current study are in broad agreement with the rod-shape micelles previously reported.[28,29] Cylindrical micelles investigated by small angle neutron scattering have been considered as a stage before spherical micelles in mixtures of glycocholate and egg-phosphatidylcholine.[29] Lamellar (L) phases were occasionally observed with the characteristic regularly stacked smooth lamellae (Figure 6A, indicated by white arrows). In some cases these lamellae were bending, forming a notch along the lamellae (indicated by an asterisk).

The dominant structures in this sample were faceted vesicles (Figure 6C, indicated by a black arrow) and vesicles containing deformed internal structures (Figure 6C, indicated by white arrows). The uneven morphology of these bilayers advocates that the formation of such structures is a dynamic process. The vesicles appear to be nonaggregated which can be attributed to their anionic character as has been demonstrated previously by surface charge measurements.[10,11]

Micellar$_{early}$ Sample. Cryo-TEM images of the intermediate colloidal products from the Micellar$_{early}$ samples are shown in Figure 7. Clusters of oil droplets (Figure 7A, indicated by a white arrow), with diameters up to 100 nm originating from the liquid meal, were present in the medium. They have similar comparable diameters, suggesting some protection from coalescence. Occasionally oil droplets tended to be aligned in regions located to the edges of plate-like structures (data not shown), suggesting an interfacial tension between the droplets and these plates in a similar manner to those previously reported.[10] Bilayer fragments (Figure 7B, indicated by a black arrow), ruptured vesicles (Figure 7C, indicated by a white arrow), and unilamellar vesicles (Figure 7C, indicated by a white arrow) with a vesicle diameter up to 60 nm coexisting with spherical micelles as "black dots" (Figure 7B,C, indicated by the letter M) were frequently observed.

■ DISCUSSION

Micelles. Spherical micelles are in abundance throughout the whole process. Our previous *in vitro* data are in agreement
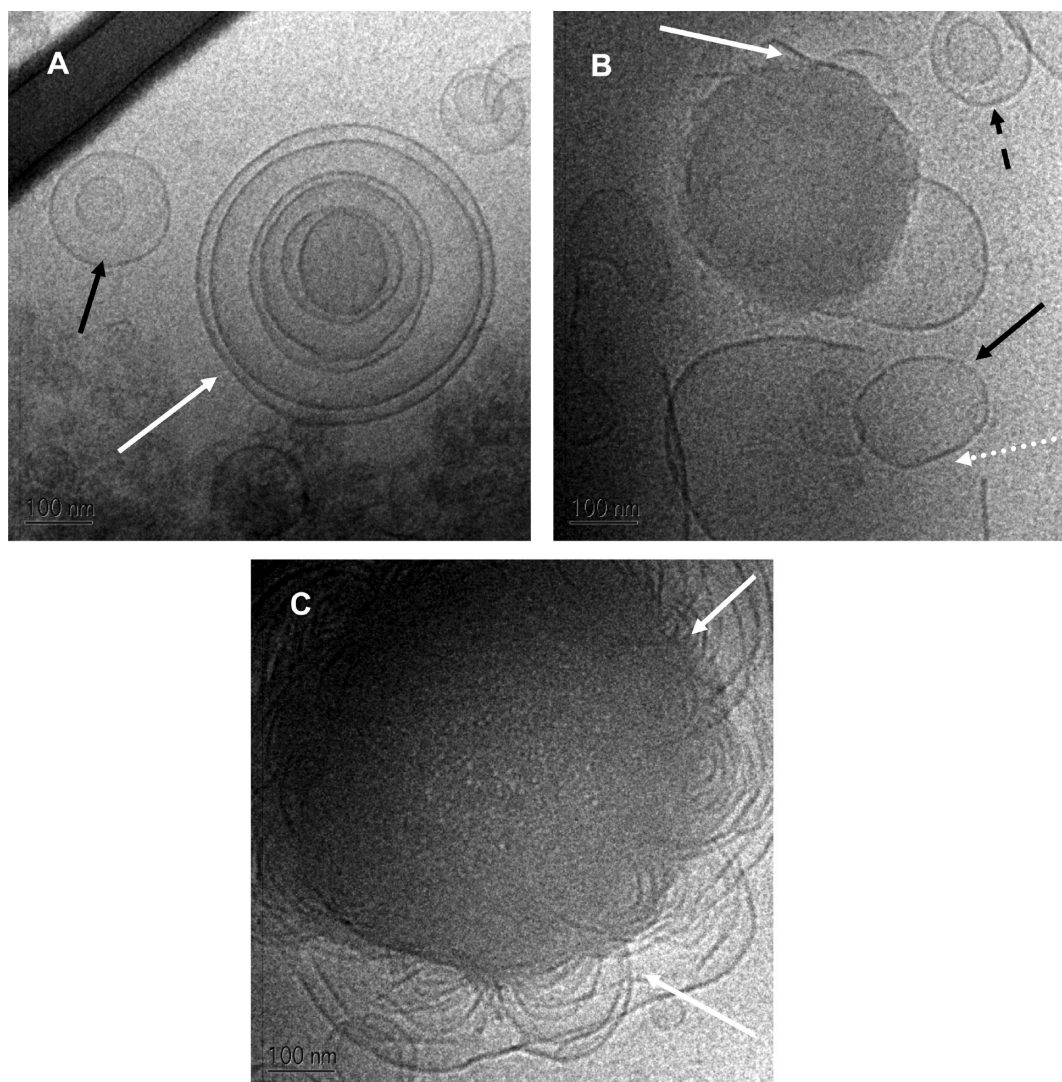
Figure 4. Cryo-TEM images of the Aspirate$_{1h}^{ave,comp}$ sample. (A) A bilamellar vesicle (indicated with a black arrow) and a multilamellar vesicle (indicated by a white arrow). (B) A unilamellar vesicle (indicated by a black arrow), bilamellar vesicle (indicated by a dashed black arrow), and ruptured vesicle (indicated by a dashed white arrow) coexisting with an oil droplet with bilayer (indicated by a white arrow) closely located to their surface suggesting the lipolytic product phases accumulated on its surface. The bar represents 100 nm. (C) Oil droplet protrusions (bilayers) emerged from it (indicated by white arrows).

with this observation.[10,14] On the contrary, thread-like micelles are a rather elusive intermediate colloid phase since their presence is documented only in the Aspirate$_{early}$ sample (Table 2). Recently, thread-like micelles were visualized by Cryo-TEM *in vitro* in a mixture containing biorelevant media with PC/BS (phosphatidylcholine/bile salts) and LP/BS (lipolytic products/bile salt) ratios of 0.25 and 2.33, respectively.[13] In previous studies, such structures have been identified in systems composed solely from BS and PC in ratios of PC/BS of 1.12.[29] In the current study, in the Aspirate$_{early}$ sample, the PC/BS and LP/BS ratios (Table 1) were 0.43 and 1.99, respectively, which are in broad agreement with the previous reports.[13,29] However, it should be emphasized that all previous studies were conducted in controlled conditions close to equilibrium, not allowing a direct comparison with the results obtained in the nonequilibrium conditions of the current study.

Multi- and Unilamellar Structures. At 1 h after meal administration, faceted vesicles and multivesicular structures were the dominating structures in the total content phase sample (Table 2), advocating that these vesicles were

metastable phases finally transformed either to micelles or well-defined vesicles (multi- or unilamellar), which were present in all samples tested. The presence of bilayer fragments in all samples corroborates the suggestion that these fragments were gradually detached from the multivesicular and faceted vesicles to form micelles and/or unilamellar vesicles. Previously, visualization studies using freeze fracture electron microscopy (FFEM) have identified the formation of vesicles and multilamellar lipolytic products both *in vitro* and in killfish intestinal lumen when the ratio of LP/BS increases beyond 1.0[5]. Similarly, multivesicular and faceted structures in the current study were frequently visible (Figures 4 and 5) when the ratios of LP/BS exceeded 1.0 (Table 1). Previously small-angle X-ray scattering measurements combined with the *in vitro* dynamic lipolysis model revealed the formation of a lamellar phase and a hexagonal phase due to the hydrolysis of a SNEDDS formulation.[14] Whether or not these structures visualized in the current study possess hexagonal or cubic configuration cannot be answered with the current data. In model studies of fat digestion *in vitro* a reversed micellar L2
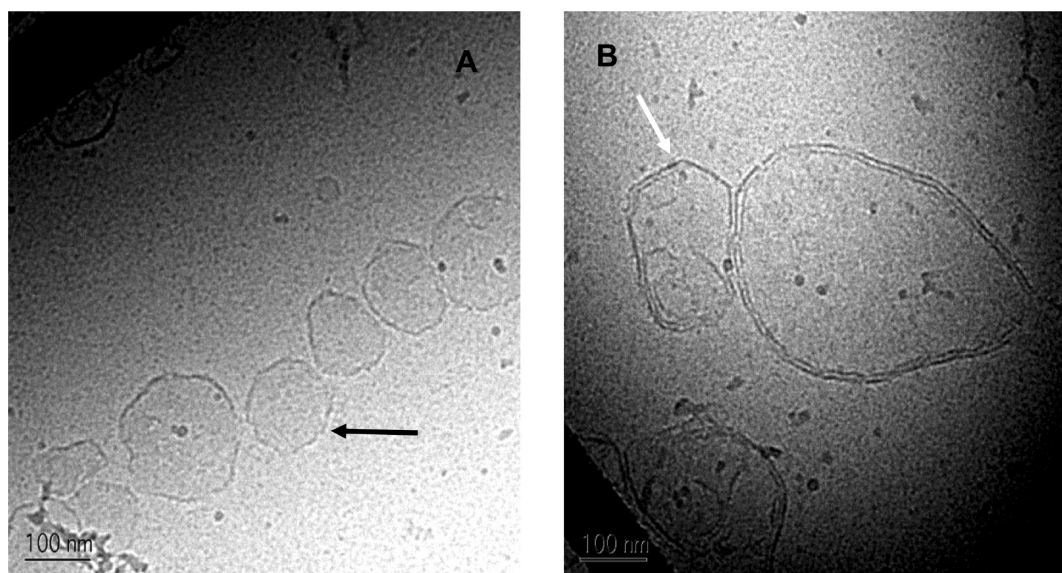
Figure 5. Cryo-TEM images of the $Micellar_{1h}^{ave,comp}$ sample. (A) Perforated vesicles (indicated by a black arrow). (B) Faceted vesicles (indicated by a white arrow).

phase was identified using FFEM and X-ray diffraction at high LP/BS ratios.[30,31] In the current study there was no evidence of such phases even at the end of the lipolysis when high LP/BS ratios were obtained.

Previously, the size distribution of the produced vesicles during the lipid digestion measured by means of FFEM in killfish[5] revealed particles between 20 and 100 nm with a small fraction exhibiting diameter larger than 150 nm which is close to particle size diameters visualized in the current study (both with Cryo-TEM and AFM).

Oil Droplets. Submicrometer emulsion droplets were visible in $Aspirate_{1h}^{ave,comp}$ and $Micellar_{early}$ samples. The inability to visualize any oil droplets in the $Aspirate_{early}$ sample could be attributed to the possibility that primarily oil droplets with particles >1 μm in diameter pass from the stomach into the duodenum (early, after meal administration). Such sizes are much larger than that accessible by Cryo-TEM (<1.0 μm). In addition in $Aspirate_{early}$ samples the micellar phase is diluted with other phases, whereas in the specific aspirated sample the triglycerides content is low (0.026 mM, Table 1), which decreases the possibility of formation of many oil droplets.

In the $Micellar_{early}$ phase, although the triglyceride content was minimal (Table 1, <LOD), some small oil droplets (less than 100 nm) could be detected in the sample (Figure 7). This rather unexpected observation might be explained in terms of the properties of these droplets. Due to their small size they might have been up-concentrated during the ultracentrifugation process and possibly migrated to the $Micellar_{early}$ phase.

With the progress of lipolysis the particle size of the produced oil droplets in the duodenum increases,[21] thus impeding their direct observation. In parallel, the proportion of smaller oil droplets increases, enabling their direct visualization ($Aspirate_{1h}^{ave,comp}$ sample), as shown in Figure 4. On the other hand, the extremely low amount of triglycerides present in the $Micellar_{1h}^{ave,comp}$ sample (Table 1, <LOD) could be the reason for not detecting any oil droplets in this sample.

The current findings do not give any evidence against the occurrence of larger oil droplets, and their existence cannot be ruled out.

Further AFM analysis of the samples did not reveal vesicles >1 μm corroborating the Cryo-TEM findings, given the AFM can image a maximum height of ca. 16 μm (max. z-range).

The coexistence of oil droplets and unilamellar vesicles with micelles to the aqueous micellar phases further supports the observations of Hernell et al.[6] that the existence of a clear micellar phase is quite rare under physiological conditions as evident from the Cryo-TEM analysis. In addition, the AFM studies further fortify the presence of other structures in the micellar phase as was demonstrated from the Cryo-TEM studies previously.

Plate-Like Structures. Finally, plate-like structures were visible in the $Micellar_{early}$ sample. Such structures have been identified previously during the *in vitro* digestion of a self-nano emulsifying drug delivery system (SNEDDS) formulation.[10,11] The plates appear to be stacked upon one another, and their origin has been attributed to the pancreatin preparation *in vitro*. Their origin merits further investigations of the pending question of whether these structures are related to the formation of cholesterol crystals. It would be of particular interest to visualize intestinal fluids equilibrated with different amounts of cholesterol and its role to colloidal structures and solubilization of drugs.

Membrane Dynamics. The unevenness of the membranes accompanied with the extensive perforation is more pronounced in the $Aspirate_{early}$ sample compared with the $Aspirate_{1h}^{ave,comp}$ sample. Furthermore, the postulated membrane roughness arising from these multivesicular structures could be attributed to the nonequilibrium conditions with the $Aspirate_{early}$ compared with the $Aspirate_{1h}^{ave,comp}$ sample, where the fat digestion has almost been completed. The size and shapes observed were highly dependent on the progress of digestion. The buildup of these structures is observed at the beginning of the process which is consistent with lipolytic product lamellae and vesicles being expected to occur as intermediates in fat digestion.[5,6] With the progress of lipolysis, the structures were more spherical and shifted towards smaller vesicles. A previous work demonstrated the same sequence of events for as long as for 30 min under low and high ratios of PC/BS using the *in vitro* digestion model.[10,11] The present
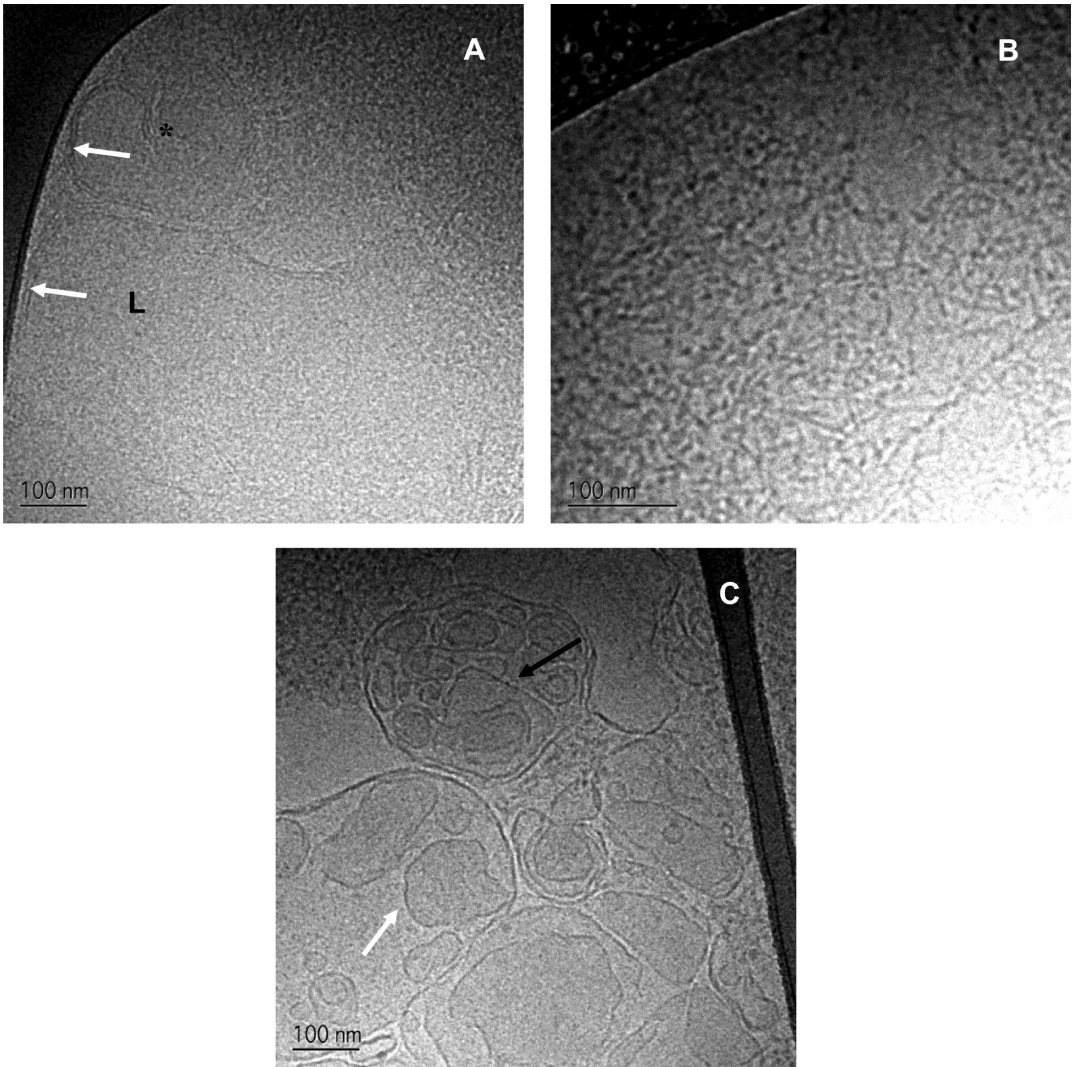
Figure 6. Cryo-TEM images of sample. (A) Spherical micelles ca. 10 nm (indicated as black dots) and lamellar phases (L) indicated by white arrows with a deep notch (indicated by an asterisk). (B) Thread-like micelles ca. 30 nm [in length]. (C) Faceted vesicles (indicated by a black arrow) coexisting with multivesicular structures with internal deformation (indicated by a white arrow).

Table 2. Cryo-TEM Observations in HIFs[a]

		observations			
sample	oil droplets	micelles (spherical/thread like)	faceted vesicles/deformed structures	vesicles (uni, bi-, multilamellar)	fragments/plate-like structures
Aspirate$_{1h}^{ave,comp}$	○	● (s)		□ (all types)	○ (fragm)
Micellar$_{1h}^{ave,comp}$		● (s)	○ (fv)	□ (uni-)	○ (fragm)
Aspirate$_{early}$		● (s), ● (tl)	● (fv), ● (ds)		○ (fragm)
Micellar$_{early}$	□	● (s)		□ (uni-)	○ (fragm), ○ (plates)

[a] ●, abundantly present; □, fairly present; ○, occasionally present; fragm: fragments, fv: faceted vesicles, ds: deformed structures, s: spherical, tl (thread-like), uni: unilamellar.

study, performed under *ex vivo* conditions, confirms and extends these findings. Finally, in the Aspirate$_{1h}^{ave,comp}$ sample, contrary to the Aspirate$_{early}$ sample, faceted objects were almost absent, while intact and well-defined vesicles were the prevailing structures. Additionally, the smaller number density of the colloidal structures present in the micellar phase samples, as compared with the total phase samples, reflects the lower concentration of lipid material in these phases.

Summary of the Visualization Studies. Summarizing the results from this study, we can conclude the following:

Lipolytic products (multivesicular, faceted vesicles, bilayer fragments) were produced with LP/BS ≥ 1.9 (Table 1), which is in good agreement with FFEM studies of lipolytic products reported previously.[5]

Unilamellar vesicles in abundance, and occasionally bilamellar and trilamellar vesicles ranging from 50 to 200 nm, were observed in all samples. This is consistent with the proposed hypothesis that during lipid digestion oligolamellar vesicles, originating from the lamellar liquid crystals formed at emulsion-water interfaces, are gradually detached and dispersed in the
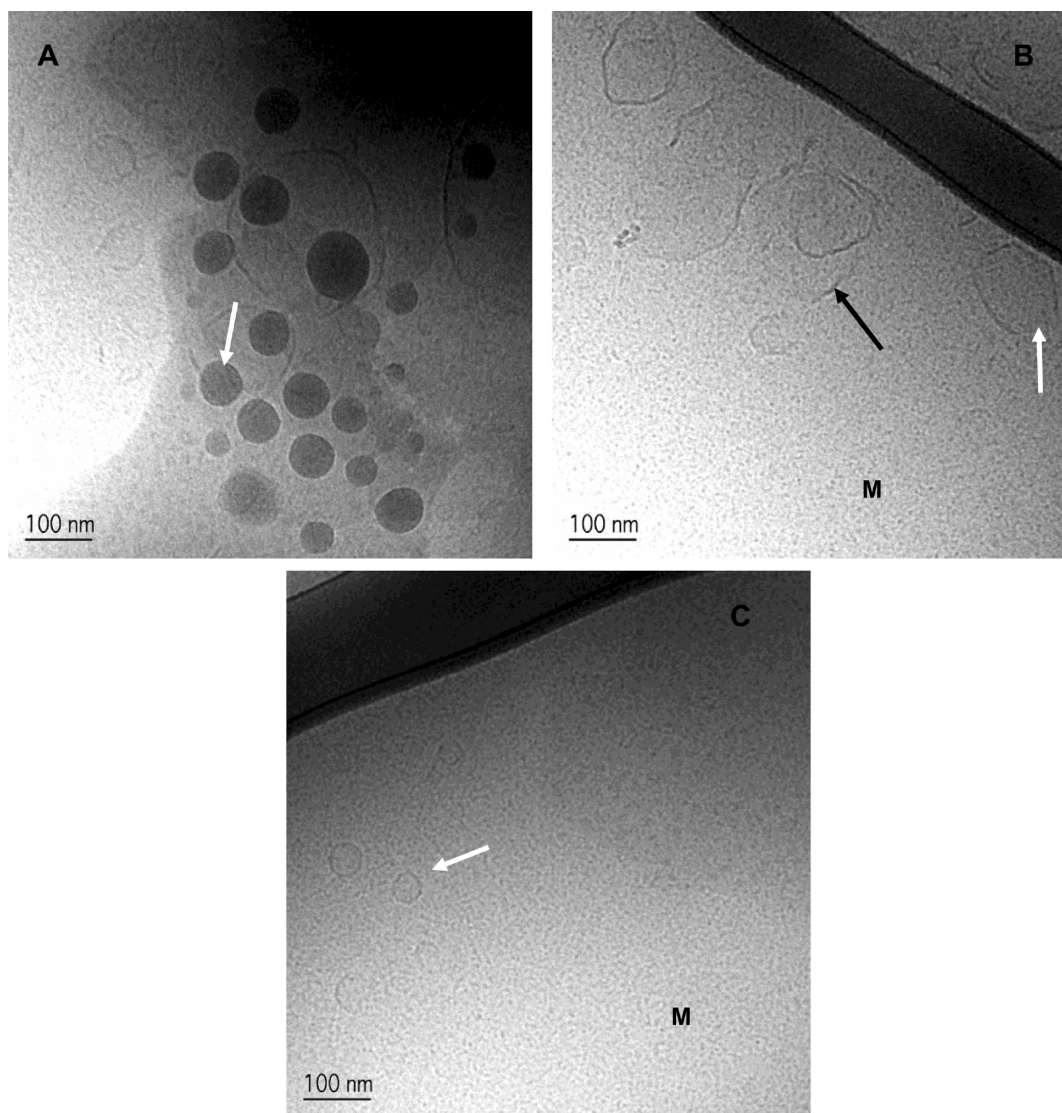
Figure 7. Cryo-TEM images of the Micellar$_{early}$ sample. (A) Cluster of oil droplets (indicated by a white arrow). (B) Ruptured vesicles (indicated by a black arrow) coexisting with bilayer fragments (indicated by a white arrow). (C) Micelles are depicted with the letter M, and unilamellar vesicles are indicated by the indicated white arrow.

medium. The observations and the values obtained in the current study are in broad agreement with the values reported using quasielastic light scattering (QELS) analysis by Hernell et al. previously.[6]

Using visualization techniques (Cryo-TEM and AFM), the current study unequivocally demonstrates, for the first time, the presence of other structural features (unilamellar vesicles, oil droplets, and faceted vesicles) in the aqueous micellar phase, isolated by ultracentrifugation, which were not previously identified using the QELS method.[6]

Spherical micelles (ca. 10 nm) were identified throughout the whole process in broad agreement with previous studies.[6,13] Thread-like micelles were visible as well; however, they appear to be rather short-lived intermediates as they were identified only in one sample.

Our observations (faceted vesicles, multivesicular structures with internal deformations) are in agreement with previous findings where FFEM was employed to visualize lipolytic products formed in the intestine killfish[5] and QELS analysis of HIFs revealing the existence of multilamellar structures,[5]

unilamellar vesicles, and mixed micelles.[6] Hernell et al.[6] have demonstrated that a pure micellar phase of duodenal contents is a very rare condition as more structural features are usually present.

In the current study, these primordial structural features (faceted vesicles, multivesicular formation with internal structures, open vesicles, and bilayer fragments) could be the "feeding material" for the formation of the micelles and unilamellar vesicles following a similar mechanism as previously reported.[5,6]

■ CONCLUSIONS

Intermediate colloidal phases produced during the *in vitro* digestion of lipid-based formulations[10,11] or direct visualization of lipolytic products[11−13] are in agreement with the structural features visualized in this work. The current study offers insights toward the microstructural elucidation of vesicular assemblies and the structural pathway of these intermediates during fat digestion. The fact that other structural features (unilamellar and faceted vesicles) than micelles are present in

the micellar phase, the presence of plate-like structures, and the fact that in the progress of lipolysis, the structures are becoming more spherical and shifted towards smaller vesicles advocating that indeed, lipolysis is a dynamic process; all such information is important in shedding light on the underlying mechanisms during fat digestion. Furthermore, it underlines the precious need of complementary studies of colloidal phases of pathological composition and nature (e.g., cystic fibrosis, Crohn's disease, celiac disease). Intermediates and their transitions are essential for an understanding of the solubilization of poorly soluble drugs in the intestine and will also enable a more rational development of lipid-based drug delivery systems aimed at the oral delivery of lipophilic drugs.

■ AUTHOR INFORMATION

Corresponding Author

*Mailing address: Aristotle University of Thessaloniki, Department of Pharmaceutical Technology, School of Pharmacy, 54124, Greece. E-mail: dfatouro@pharm.auth.gr. Tel.: +302310997653. Fax: +302310997652.

■ REFERENCES

(1) Hofmann, A. F.; Borgstrom, B. Physico-chemical state of lipids in intestinal content during their digestion and absorption. *Fed. Proc.* **1962**, *21*, 43−50.

(2) Hofmann, A. F.; Borgstrom, B. Intraluminal phase of fat digestion in man-lipid content of micellar and oil phases of intestinal content obtained during fat digestion and absorption. *J. Clin. Invest.* **1964**, *43*, 247−257.

(3) Patton, J. S.; Carey, M. C. Watching fat digestion. *Science* **1979**, *204*, 145−148.

(4) Patton, J. S.; Vetter, R. D.; Hammosh, M.; Borgstrom.; Lindstrom, M.; Carey, M. C. The light-microscopy of triglyceride digestion. *Food Microstruct.* **1985**, *4*, 29−41.

(5) Rigler, M. W.; Honkanen, R. E.; Patton, J. S. Visualization by freeze fracture, *in vitro* and *in vivo*, of the products of fat digestion. *J. Lipid Res.* **1986**, *8*, 836−857.

(6) Staggers, J. E.; Hernell, O.; Stafford, R. J.; Carey, M. C. Physical−chemical behaviour of dietary and biliary lipids during intestinal digestion and absorption. 1. Phase behaviour and aggregation states of model lipids systems patterned after aqueous duodenal contents of healthy adult human beings. *Biochemistry* **1990**, *29*, 2028−2040.

(7) Hernell, O.; Staggers, J. E.; Carey, M. C. Physicochemical behaviour of dietary and biliary lipids during intestinal digestion and absorption. 2. Phase behaviour and aggregation states of luminal lipids during duodenal fat digestion in health adult human beings. *Biochemistry* **1990**, *29*, 2041−2056.

(8) Kossena, G. A.; Boyd, B. J.; Porter, C. J. H.; Charman, W. N. Separation and characterization of the colloidal phases produced on digestion of common formulation lipids and assessment of their impact on the apparent solubility of selected poorly water-soluble drugs. *J. Pharm. Sci.* **2003**, *92*, 634−648.

(9) Kossena, G. A.; Charman, W. N.; Boyd, B. J.; Porter, C. J. H. Influence of the intermediate digestion phases of common formulation lipids on the absorption of a poorly water-soluble drug. *J. Pharm. Sci.* **2005**, *94*, 481−492.

(10) Fatouros, D. G.; Bergenstahl, B.; Müllertz, A. Morphological observations on a lipid based drug delivery system during *in vitro* digestion. *Eur. J. Pharm. Sci.* **2007**, *31*, 85−94.

(11) Fatouros, D. G.; Walrand, I.; Bergenstahl, B.; Müllertz, A. Colloidal structures in media simulating intestinal fed state conditions with and without lipolysis products. *Pharm. Res.* **2009**, *26*, 361−373.

(12) Fatouros, D. G.; Walrand, I.; Bergenstahl, B.; Müllertz, A. Physicochemical characterization of simulated intestinal fed-state fluids containing lyso-phosphatidylcholine and cholesterol. *Dissol. Technol.* **2009**, *16*, 47−50.

(13) Kleberg, K.; Jacobsen, J.; Fatouros, D. G.; Müllertz, A. Biorelevant media simulating fed state intestinal fluids: colloid phase characterization and impact on solubilization capacity. *J. Pharm. Sci.* **2010**, *99*, 3522−3532.

(14) Fatouros, D. G.; Roshan Deen, G.; Arleth, L.; Bergenståhl, B.; Nielsen, F. S.; Pedersen, J. S.; Müllertz, A. Structural changes of self nano emulsifying drug delivery systems during *in vitro* lipid digestion monitored by small angle x-ray scattering. *Pharm. Res.* **2007**, *24*, 1844−1853.

(15) Salentinig, S.; Sagalowicz, L.; Leser, M. E.; Tedeschi, C.; Glatter, O. Transitions in the internal structure of lipid droplets during fat digestion. *Soft Matter* **2011**, *7*, 650−661.

(16) Rube, A.; Klein, S.; Mader, K. Monitoring of in vitro fat digestion by electron paramagnetic resonance spectroscopy. *Pharm. Res.* **2006**, *9*, 2024−2029.

(17) Day, J. P.; Rago, G.; Domke, K. F.; Velikov, K. P.; Bonn, M. Label-free imaging of lipophilic bioactive molecules during lipid digestion by multiplex coherent anti-Stokes Raman scattering microspectroscopy. *J. Am. Chem. Soc.* **2010**, *132*, 8433−8439.

(18) Dufrene, Y. F.; Boland, T.; Schneider, J. W.; Barger, W. R.; Lee, G. U. Characterization of the physical properties of model biomembranes at the nanometer scale with the atomic force microscope. *Faraday Discuss.* **1998**, *111*, 79−94.

(19) Dubochet, J.; Adrian, M.; Chang, J.; Homo, J. C.; Lepault, J.; McDowell, A. W.; Schultz, P. Cryo-electron microscopy of vitrified specimens. *Q. Rev. Biophys.* **1988**, *21*, 129−228.

(20) Vertzoni, M.; Markopoulos, C.; Symilllides, M.; Goumas, C.; Imanidis, G.; Reppas, C. Lumenal lipid phases after administration of a triglyceride solution of danazol in the fed state and their impact on the flux of danazol via the intestinal mucosa. *Mol. Pharmaceutics*, revised.

(21) Armand, M.; Borel, P.; Pasquier, B.; Dubois, C.; Senft, M.; Peyrot, J.; Salducci, J.; Lafont, H.; Lairon, D. Characterization of emulsions and lipolysis of dietary lipids in the human stomach. *Am. J. Phys.* **1994**, *266*, G372−G381.

(22) Vertzoni, M.; Archontaki, H.; Reppas, C. Determination of intralumenal individual bile acids by HPLC with charged aerosol detection. *J. Lipid Res.* **2008**, *49*, 2690−2695.

(23) Diakidou, A.; Vertzoni, M.; Goumas, K.; Söderlind, E.; Abrahamsson, B.; Dressman, J. B.; Reppas, C. Characterization of the contents of ascending colon to which drugs are exposed after oral administration to healthy adults. *Pharm. Res.* **2009**, *26*, 2141−2151.

(24) Dressman, J. B.; Vertzoni, M.; Goumas, K.; Reppas, C. Estimating drug solubility in the gastrointestinal tract. *Adv. Drug Delivery Rev.* **2007**, *59*, 591−602.

(25) Balashev, K.; Atanasov, V.; Mitewa, M.; Petrova, S.; Bjørnholm, T. Kinetics of degradation of dipalmitoylphosphatidylcholine (DPPC) bilayers as a result of vipoxin phospholipase A2 activity: An atomic force microscopy (AFM) approach. *Biochim. Biophys. Acta* **2011**, *80*, 191−198.

(26) Mel'nikova, Y. S.; Mel'nikov, S. M.; Löfroth, J. E. Physico-chemical aspects of the interaction between DNA and oppositely charged mixed liposomes. *Biophys. Chem.* **1999**, *81*, 125−141.

(27) Waninge, R.; Kalda, E.; Paulsson, M.; Nylander, T.; Bergenstahl, B. Cryo-TEM of isolated milk fat globule membrane structures in cream. *Phys. Chem. Chem. Phys.* **2004**, *6*, 1518−1523.

(28) Hjelm, R. P.; Thiyagarajan, P.; kan-Onyuksel, H. Organization of phosphatidylcholine and bile salt in rodlike mixed micelles. *J. Phys. Chem.* **1992**, *96*, 8653−8661.

(29) Walter, A.; Vinson, P. K.; Kaplun, A.; Talmon, Y. Intermediate structures in the cholate-phosphatidylcholine vesicle-micelle transition. *Biophys. J.* **1991**, *60*, 1315−1325.

(30) Lindström, M.; Ljusberg-Wahren, H.; Larsson, K; Borgström, B. Aqueous lipid phases of relevance to intestinal fat digestion and absorption. *Lipids* **1981**, *16*, 749−754.

(31) Gulik-Krzywicki, T.; Larsson, K. An electron microscopy study of the L2-phase (microemulsion) in a ternary system: Triglyceride/monoglyceride/water. *Chem. Phys. Lipids* **1984**, *35*, 127−132.